# DEVELOPING A GEOMETRIC DEFORMABLE MODEL FOR RADAR SHAPE INVERSION

*Alper Yildirim, Anthony Yezzi*

Georgia Institute of Technology
School of Electrical and Computer Engineering
Atlanta, GA

**ABSTRACT**

In this paper, we develop a radar-based dense scene reconstruction model that extracts shape information embedded in the radar return signal. Our method uses a deformable shape evolution approach which seeks to match the received signal to a computed forward model based on the evolving shape. This allows us to directly incorporate geometric considerations of the shape into the problem formulation, such as smoothness and self-occlusions. Iterations start with an initial shape which is gradually deformed until its image under the forward model gets sufficiently close to the actual measured signal. For this purpose, we employ the technique of stretch processing to extract geometric properties of the shape from radar return signal. This yields a smooth and purely geometric cost functional by which shape inversion can be robustly performed via gradient-based minimization algorithms. Synthetic simulations with a polygonal shape model show the promise of this type of approach on some challenging shapes.

***Index Terms*—** Shape inversion, Radar imaging

## 1. INTRODUCTION

Vision systems are becoming more and more essential in robotic systems because of the rich information they can provide about their environment. Especially for robots that are to navigate in cluttered environments, awareness of the scene structure is of great importance as it is usually the main limiting factor on robot motion. Inferring such structure using visual cues from camera images is a natural approach which mimics the way we sense the world with our eyes. This is an old and well established area of research in computer vision known as structure from motion or multiview stereo reconstruction, including methods based on deformable shape models [1] [2]. However, stereo vision systems have inherent fragility in the case of low ambient light or in the presence of obstructing factors for the visible light spectrum, such as rainy and foggy weather or smoke. As a result, alternative sensing modalities can often be required for the applications where these conditions are present.

Radar systems are immune to many factors which challenge visual sensors as they have good penetration capabilities through certain mediums, air, water etc. [3] These systems are essential especially for airborne and spaceborne imaging applications where light rays can easily be blocked by the clouds or the thick layer of air between the antenna and ground scene. Radar imaging is mostly performed with an apparatus known as Synthetic aperture radar (SAR)[4][5][6][7]. A SAR system is usually composed of a small antenna or antennas attached to a moving platform which takes measurements of the scene from different viewpoints. These measurements are then used to synthesize a high resolution image of the scene. The scene is modelled as an array of scatterers where a reflectivity (intensity) value is assigned to each scatterer as a result of the synthesis.

SAR imaging does not presently have an explicit notion of shape that can easily be leveraged to exploit geometric prior information about object shape. For example, we know that the surfaces of scene objects usually exhibit some level of smoothness which could potentially be used to regularize the problem. Another important aspect of object geometry is self-occlusion where certain parts of the object can block the view of other parts. Occlusion modelling is especially critical for close range applications where the visible parts of the object can drastically change with respect to the view-point. Modelling such considerations can be of great help to enhance the quality of estimation.

In this paper, we propose a generative model based evolution approach for radar by which we can directly incorporate object geometry into the problem formulation. In Section 2, we formulate the forward model to be used to estimate the received signal given the shape. Second, we outline an iterative inversion scheme based on a deformable shape model. In Section 3, simulations for different cases are presented. In section 4, results are discussed.

## 2. DEFORMABLE SHAPE MODEL

Reflected radar signal is a highly non-linear function of shape where the inversion problem can only be attacked by an iterative approach. We first need a forward model to compute the expected return signal given a candidate shape for the object. We then measure the discrepancy between this computed signal and actual measured signal and use the residual error value to update our guess for the object so that we have a decreased

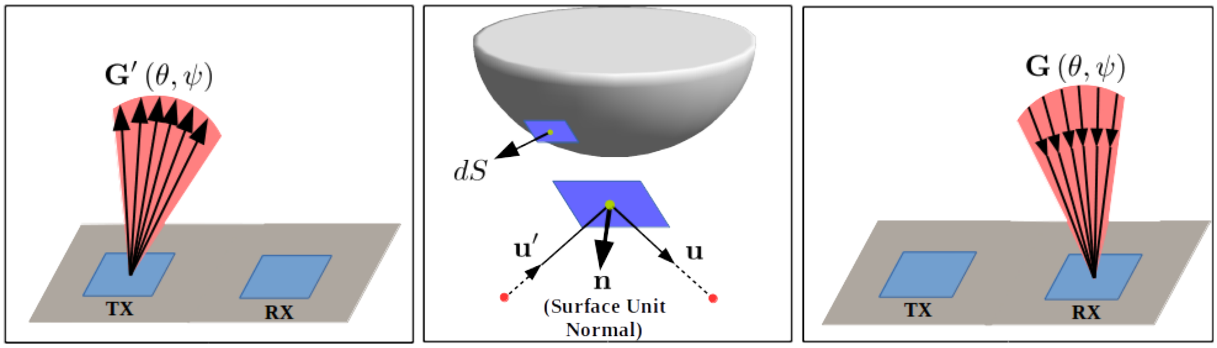


**Fig. 1**. Our Forward Model, Transmittance (left), Receivence (right), EM wave-object interaction (center)

error value in the next step.

### 2.1. Forward Model

Our forward model computes what is expected from the receiver antenna given a transmitted waveform and an object shape (and reflectivity). On the antenna side, we model the transmitter and receiver as point antennas with directional gains. For the object, we assume Lambertian surface reflectivity where incoming radiation is scattered via a cosine power law. From a small surface patch of area $dS$, the received signal is modelled as:

$$dQ_c(t) = \frac{G'G(\mathbf{u}'\cdot\mathbf{n})(\mathbf{u}\cdot\mathbf{n})}{R'^2R^2} f\left(t - \frac{R+R'}{c}\right) dS \quad (1)$$

where $G'$ and $G$ are antenna gain values for the transmitter and receiver in a given direction, $\mathbf{u}'$ and $\mathbf{u}$ are the unit ray directions connecting transmitter and receiver antennas to the object, $R'$ and $R$ are the lengths of these rays and $\mathbf{n}$ is the unit normal vector of the object at the given point, respectively. $f(t)$ is the transmitted waveform which is mostly a frequency-modulated complex exponential. Squared ray lengths in the denominator model the decay of power density with wave propagation (inverse-square law). Our forward model is depicted in the Fig. 1.

For a given antenna position, all of the visible points on the surface will contribute to this measurement which makes the total measured signal:

$$Q_c(t) = \int_S \frac{G'G(\mathbf{u}'\cdot\mathbf{n})(\mathbf{u}\cdot\mathbf{n})}{R'^2R^2} f\left(t - \frac{R+R'}{c}\right) dS \quad (2)$$

where $S$ is the set of visible points visible to both transmitted and receiver antenna.

### 2.2. Inverse Model

Our purpose is to estimate the surface shape from the measured signal, which requires inverting the forward model. However, this model is highly nonlinear and inverting it is an inherently ill-posed operation. That's why we start with an initial shape and let this shape evolve such that its image under the forward model gets closer to the actual measured signal, balanced by additional geometric priors under a designed cost functional, with successive iterations.

Design of the cost functional to be used in an iterative minimization procedure is tricky for radar applications, especially when high frequency waveforms are used. We need a cost functional that is not only rich in shape information but at the same time independent as possible from the structure of the waveform being used. Naive choices for this design can bring the oscillatory structure of the waveform into the cost functional. This causes the energy manifold to be full of local minima, making robust shape inversion impossible or impractical. Accordingly, the design of the cost functional is the key component of our scheme. For this purpose we employ the technique known as stretch processing [8]

#### *2.2.1. Stretch Processing*

Stretch processing is a commonly used technique in the radar community to process large bandwidth signals using low sampling rates. It is a requirement for some applications as signals of large bandwidths cannot be processed directly on hardware due to the sampling rate limitations of A/D converters [9][10][11]. This is done by mixing the return signal with a time shifted replica of the transmitted signal, which results in a lower frequency signal at the mixer output that can then be sampled properly. However, a more important aspect of this process for us is that each frequency component residing in the output signal can directly be linked to a subset of surface points all of which have equal round-trip distance values. This property of stretch processing will be highly beneficial for our purposes as this indirectly gives us distribution of signal strength along the object range. For a point on the object surface, we express the received signal in Eq. 1. Choosing $f(t)$ as an LFM pulse and transforming this signal using a stretch processor, at the mixer output we obtain:

$$dh(t) = \frac{G'G(\mathbf{u}'\cdot\mathbf{n})(\mathbf{u}\cdot\mathbf{n})}{R'^2R^2} \Phi(t_r)\, e^{i4\pi\alpha(t_r-t_h)t} dS \quad (3)$$

$$\Phi(t_r) = e^{i2\pi\left(f_c(t_r-t_h)-\alpha\left(t_r^2-t_h^2\right)\right)} \quad (4)$$

$$t_r = \left(R'+R\right)/c \quad (5)$$

where $\alpha$ is the chirp rate, $f_c$ is the carrier frequency, $t_r$ and $t_h$ are the delays of received and replica signals with respect to the transmitted signal, respectively. Since the output signal of the stretch processor will be the linear combination of these infinitesimal components coming from visible points along the object surface, the total output for the object becomes:

$$h(t) = \int_S \frac{G'G\left(\mathbf{u}'\cdot\mathbf{n}\right)\left(\mathbf{u}\cdot\mathbf{n}\right)}{R'^2 R^2}\Phi\left(t_r\right)e^{i4\pi\alpha(t_r - t_h)t}dS \quad (6)$$

where $S$ denotes the visible part of the object surface with respect to the transmitter and receiver. It should be noted that $\Phi(t_r)$ is a pure phase term that does not have any time dependency.

#### 2.2.2. *Feature Extraction*

The stretch processor output gives us another time dependent oscillatory signal with respect to both $t$ (time) and $t_r$ (round-trip delay). Our purpose is to remove these dependencies such that we can formulate our cost functional in terms of purely geometric quantities. For this purpose, we will find it useful to express Eq. 6 in terms of another integral with a frequency measure. Assuming an infinitely long transmitted pulse, we would have a finite support frequency spectrum where minimum ($f_{min}$) and maximum ($f_{max}$) frequencies are specified by minimum and maximum round-trip distance values of the visible portion of the object surface. $h(t)$ could then be expressed as a Fourier synthesis:

$$h(t) = \int_{f_{min}}^{f_{max}} H(\zeta)e^{i2\pi\zeta t}d\zeta \quad (7)$$

At this point we define a new function $\mathcal{H}(x)$ which will happen to be the envelope of the frequency spectrum. $\mathcal{H}(x)$ is defined such that $H(x)$ can be decomposed as:

$$H(x) = \mathcal{H}(x)\Phi(t_r) \quad (8)$$

$$t_r = \frac{x}{2\alpha} + t_h \quad (9)$$

Integrands in Eq. 6 and 7 can be related to each other after cancellation which then becomes:

$$\mathcal{H}(\zeta) = \int_{S_\zeta} \frac{G'G\left(\mathbf{u}'\cdot\mathbf{n}\right)\left(\mathbf{u}\cdot\mathbf{n}\right)}{R'^2 R^2}\left\|\frac{dS}{d\zeta}\right\|ds \quad (10)$$

where the $S_\zeta$ is the set of iso-round-trip distant points that induce a signal with a constant frequency of $\zeta$ at the mixer output.

$\mathcal{H}(x)$ is almost always a smoothly changing function of object shape when certain level of regularity is assumed for the object surface. That's why we choose to define our cost functional in terms of this expression. It should be noted that this expression is almost never a physically measurable quantity (as the set $S_\zeta$ is most of the time composed of finite number of curves lying on the object surface) so we compute its integral over a frequency range and then use the average value of the integral as our feature. We partition our frequency spectrum $[f_{min}, f_{max}]$ into frequency bins and integrate the expression in Eq.10 over each frequency interval.

$$\mathcal{H}_j = \frac{1}{\Delta f_j}\int_{f_{j-1}}^{f_j}\int_{S_\zeta} \frac{G'G\left(\mathbf{u}'\cdot\mathbf{n}\right)\left(\mathbf{u}\cdot\mathbf{n}\right)}{R'^2 R^2}\left\|\frac{dS}{d\zeta}\right\|dsd\zeta \quad (11)$$

$$\Delta f_j = f_j - f_{j-1} \quad (12)$$

where superscript $j$ denotes frequency bin index. It should be emphasized that feature $\mathcal{H}_j$ does not have any waveform dependency as we desire.

### 2.3. Inversion Scheme

We will perform shape inversion mainly by using the set of geometric features we extract from the signal. There will be two sets of these, one extracted from the actual return signal ($\mathcal{H}_j$) and the other one from the evolving object ($\hat{\mathcal{H}}_j$). For the following discussion, we will use a tailored version of our formulation to a 2D case with a discrete polygonal shape representation since our simulation results will be based on this formulation. We will model our scene as a polygonal shape which is parametrized by the set of the vertex coordinates ($\mathbf{v}_k$). Object surface is then composed of line segments connecting these vertices together. A given line segment can have intersection with more than one frequency bin in which case we slice it into pieces such that each piece is contained in one frequency bin. As a result, a given frequency bin can be contributed by portions of different line segments. For $n$ vertices, a given feature $\mathcal{H}_j$ is computed as:

$$\mathcal{H}_j = \sum_{k=1}^{n}\mathcal{H}_j^k \quad (13)$$

where $\mathcal{H}_j^k$ denotes the contribution to the $\mathcal{H}_j$ brought by the line segment that connects $v_k$ to $v_{k+1}$ (takes zero value if not intersecting).

#### 2.3.1. *Cost Functional*

Our cost functional depends mainly on these two sets of features. We also add a curvature based regularizer penalty to make the evolving shape favor a certain level of smoothness. The ability to directly regularize the shape estimate in this manner is a powerful advantage of this approach. Combining these two terms yields:

$$E\left(\mathbf{v}_1, \cdots, \mathbf{v}_n\right) = \underbrace{\sum_{j=1}^{N_F}\left(\hat{\mathcal{H}}_j - \mathcal{H}_j\right)^2}_{\text{Antenna Measurement Residual}} + \underbrace{\lambda\sum_{k=1}^{n}\kappa_k^2}_{\text{Geometric Prior}} \quad (14)$$

where $N_F$ is the number of frequency bins. In the case of multiple antenna sets, residual term is additionally summed over all antenna sets. For the regularizer term, $\lambda$ is a tunable regularization coefficient and $\kappa_k$ is the discrete curvature value computed around the $k^{th}$ vertex. We define $\kappa_k$ as:

$$\kappa_k = \left\|\frac{\mathbf{v}_{k+1} - \mathbf{v}_k}{\|\mathbf{v}_{k+1} - \mathbf{v}_k\|} - \frac{\mathbf{v}_k - \mathbf{v}_{k-1}}{\|\mathbf{v}_k - \mathbf{v}_{k-1}\|}\right\| \quad (15)$$

where $\mathbf{v}_{k-1}$, $\mathbf{v}_k$, $\mathbf{v}_{k+1}$ are the 2D coordinates of consecutive vertices of our polygonal shape in counter-clockwise order.

#### 2.3.2. *Initialization*

Using an iteration based approach brings the question of how to choose an initial parameter set. Luckily our design of the

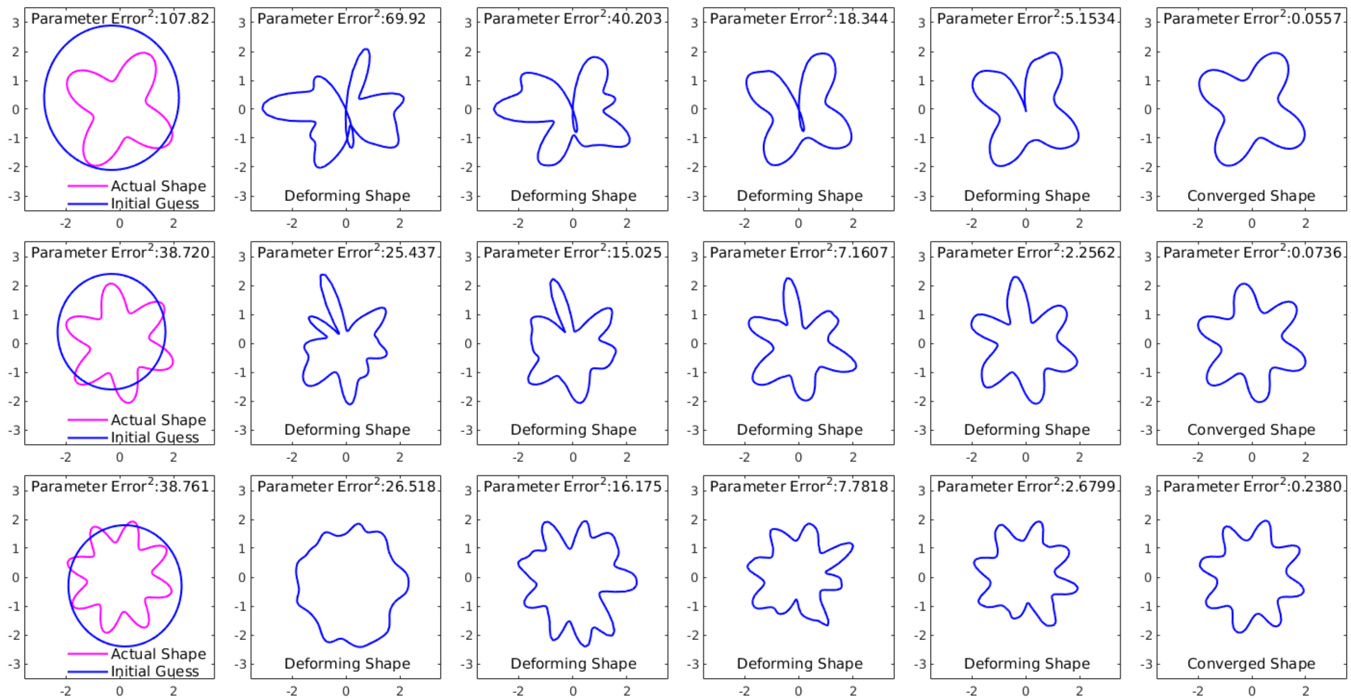


**Fig. 2**. Shape evolutions for three cases. Initial shape estimates are shown along the left column. Final converged estimates are shown along the right column and deformation process is illustrated in between. Sum of error squares for distances between the vertices of the evolving and the actual object is given at the top(polygon has 100 vertices in total). Axes units are in meters

feature set gives an easy way to come up with a close initialization. The feature set extracted from the actual measured signal naturally reveals which frequency bins have an intersection with the object where a nonzero feature value implies intersection. Triangulation of this information coming from other antennas give us a good estimate for actual object shape and placement.

### *2.3.3. Minimization*

We use Nesterov's accelerated gradient descent algorithm [12][13][14] minimize our cost functional over the vertex coordinates $(\mathbf{v}_1, \cdots, \mathbf{v}_n)$. This yields a faster convegence rate and increases robustness against shallow local minima. At each iteration, we perform a visibility analysis on the evolving shape which defines our domain of integration (different for each antenna).

## 3. SIMULATION RESULTS

We apply our inversion model to three progressively challenging 2D shapes that are modelled as polygonal objects . For each polygonal shape, we fix the angular positions of the vertices and let the shape evolve by changing their radii. Multiple antennas are placed around the object as a circular pattern with equal angular intervals between consecutive antennas.

Simulations are run for three different cases with different initial and actual shapes. For each simulation, we use 20 antennas that are circularly placed around the object where origin-antenna distance is taken as 6 meters. For each shape, we use a polygonal model with 100 vertices.

## 4. CONCLUSIONS

We propose a new model for radar based shape inversion that is using a forward model based approach since such an approach allows us to introduce geometric properties of the shape into the problem formulation. However, such an approach can be tricky when cost functional is naively chosen in terms of radar signals as these oscillations can be easily transferred to the cost functional which would make the iterative approach impractical. Thus we propose new way to design features for radar a based inversion that are purely geometric and independent of the waveform. Because of the easiness in the implementation and visualization, we choose to tailor our approach to 2D case. Simulation results are presented for different cases where even for large initial parameter error values, we see our method can effectively recover the shape of the scene.

## Acknowledgements

This material is based upon work supported by the National Science Foundation under grant no. CCF-1526848. We also thank Texas Instruments for their generous support.

## 5. REFERENCES


[1] Anthony J Yezzi and Stefano Soatto, "Structure from motion for scenes without features," in *Computer Vision and Pattern Recognition, 2003. Proceedings. 2003 IEEE Computer Society Conference on*. IEEE, 2003, vol. 1, pp. I–I.

[2] Anthony Yezzi and Stefano Soatto, "Stereoscopic segmentation," *International Journal of Computer Vision*, vol. 53, no. 1, pp. 31–43, 2003.

[3] Mark A Richards, Jim Scheer, William A Holm, and William L Melvin, *Principles of modern radar*, Citeseer, 2010.

[4] Christopher F Barnes, "Synthetic aperture radar," *Wave Theory Foundations, Analysis and Algorithms, Barnes, Powder Springs, Georgia*, 2015.

[5] William M Brown, "Synthetic aperture radar," *IEEE Transactions on Aerospace and Electronic Systems*, , no. 2, pp. 217–229, 1967.

[6] Walter G Carrara, Ron S Goodman, and Ronald M Majewski, *Spotlight synthetic aperture radar*, , 2007.

[7] Margaret Cheney, "A mathematical tutorial on synthetic aperture radar," *SIAM review*, vol. 43, no. 2, pp. 301–312, 2001.

[8] W. Caputi, "Stretch: A Time-Transformation Technique," *IEEE Transactions on Aerospace Electronic Systems*, vol. 7, pp. 269–278, Mar. 1971.

[9] Mervin C Budge and Shawn R German, *Basic RADAR analysis*, Artech House, 2015.

[10] Ihsan Ilhan, Ali Cafer Gurbuz, and Orhan Arikan, "Sparsity based robust stretch processing," in *Digital Signal Processing (DSP), 2015 IEEE International Conference on*. IEEE, 2015, pp. 95–99.

[11] Michael Schikorr, "High range resolution with digital stretch processing," in *Radar Conference, 2008. RADAR'08. IEEE*. IEEE, 2008, pp. 1–6.

[12] Yurii Nesterov, "A method of solving a convex programming problem with convergence rate o (1/k2)," in *Soviet Mathematics Doklady*, 1983, vol. 27, pp. 372–376.

[13] Weijie Su, Stephen Boyd, and Emmanuel Candes, "A differential equation for modeling nesterovs accelerated gradient method: Theory and insights," in *Advances in Neural Information Processing Systems*, 2014, pp. 2510–2518.

[14] Andre Wibisono, Ashia C Wilson, and Michael I Jordan, "A variational perspective on accelerated methods in optimization," *Proceedings of the National Academy of Sciences*, p. 201614734, 2016.